Supporting Information

Carbon dot-based ratiometric fluorescent probe for the fluorescent "on-off-on" detection of Fe^{3+} and Amitrole herbicides

Tingjie Jiang, Na Yang, Ziyi Wang, Haoran Zhang*, Na Li, Yongying Chen, Mingkai Wei, Xuejie Zhang, and Bingfu Lei*

Key Laboratory for Biobased Materials and Energy of Ministry of Education, College of Materials and Energy, South China Agricultural University, Guangzhou 510642, China

***Address correspondence to E-mail:**

tleibf@scau.edu.cn (Bingfu Lei)

hrzhang@scau.edu.cn (Haoran Zhang)

Experimental Section

1. The Construction of smartphone-based sensing platform

As illustrated in **Scheme. S1a**, the smartphone-based sensing platform is an opaque black box comprising three main components: 3D-printed accessories, solid-state sensing units, and a smartphone. The 3D-printed components were designed using *SolidWorks* software and fabricated via resin-based 3D printing technology. The smartphone is securely mounted on a bracket, ensuring that its camera precisely aligns with the sample cell. Within the device, the UV-LED light source, macro lens, filter, sample unit, and smartphone camera are compactly integrated. The macro lens enhances imaging quality, while the filter minimizes interference from the light source on fluorescence detection. The device's compact size and weight make it portable and suitable for handheld operation. The smartphone camera captures the fluorescence image of the sample, which is then processed by a smartphone application (*color picker*) to convert the fluorescence signal into digital RGB values (**Scheme. S1b**). Finally, the analyte concentration is determined based on the established mathematical relationship between analyte concentration and RGB values (**Scheme. S1c**).

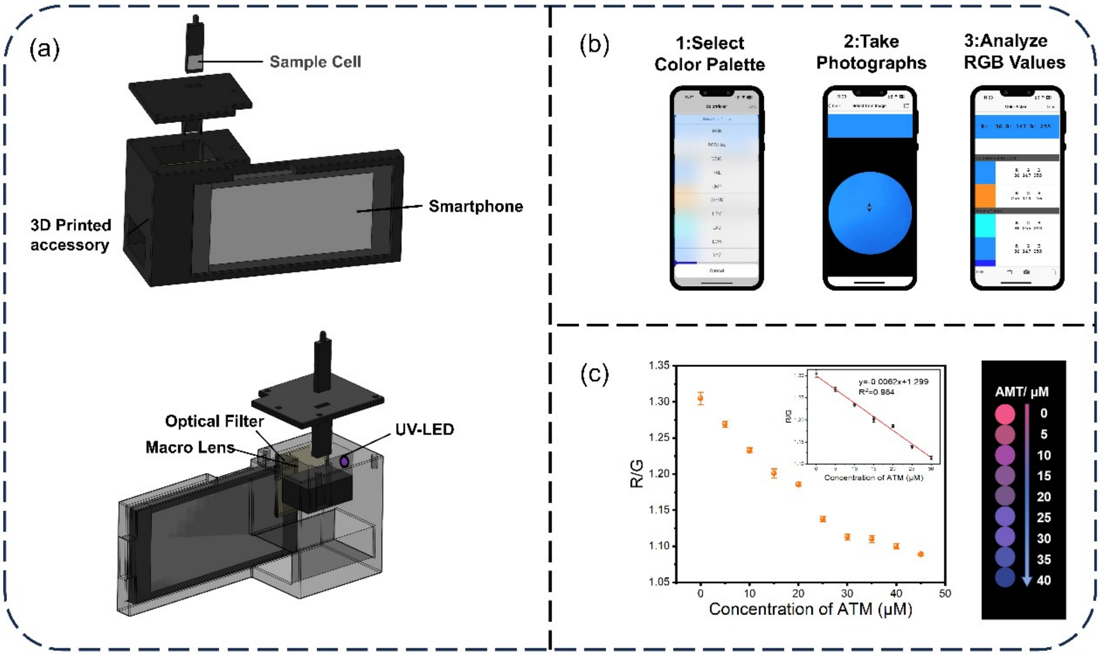

Scheme. S1 (a) Appearance and inner structure of the smartphone sensing platform. (b) Smartphone analysis process. (c) Deriving the relationship between R/G and analyte concentration.

2. The synthesis steps of the luminescence film

The specific synthesis steps were as follows: 4.8 mL polyvinyl alcohol (PVA, 5%) solution was added to 28 mL sodium alginate (SA, 2%) solution and stirred thoroughly for 1 hour. Then 3 mL (0.125 mg/mL) RF-CDs-Fe^{3+} solution was added to the above solution and stirred for 1 hour. Then 0.2 g glycerol was added to the above solution as a plasticizer. The hydrophobicity and toughness of the films were improved by crosslinking them with 0.2% calcium chloride solution. The mixture was stirred thoroughly. Finally, the above solution was poured into a culture dish, and the culture dish was placed in an oven for drying to obtain the film.

3. Calculation of the fluorescence quantum yield (QY) of RF-CDs

Choosing quinine sulfate (QY=54%, 0.1M) as the reference [1]. Dilute solutions of RF-CDs and quinine sulfate with their absorbance below 0.05 were prepared, respectively. The QY were calculated according to the below equation:

$$QY = QY_B \times I \times A_B \times n^2 / I_B \times A \times {n_B}^2 \quad (1)$$

QY and QY_B are the fluorescence quantum yield of RF-CDs and quinine sulfate, respectively. I and I_B are the integrated fluorescence intensities of RF-CDs and quinine sulfate, respectively. A and A_B are the UV-Vis absorption intensities of RF-CDs and quinine sulfate, respectively. n is refractive index of the solvent.

Supplemental Figures:

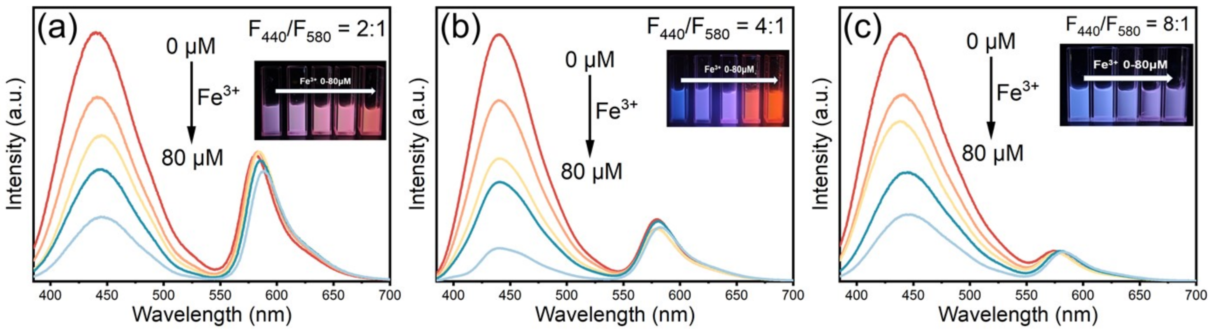

Fig. S1 The fluorescent spectra of RF-CDs with different concentrations of Fe^{3+}. The fluorescence intensity ratios (F_{440}/F_{580}) were adjusted to (a) 2:1, (b) 4:1, (c) 8:1. The insets in each figure are respectively photos of the corresponding fluorescent solutions excited at 365 nm.

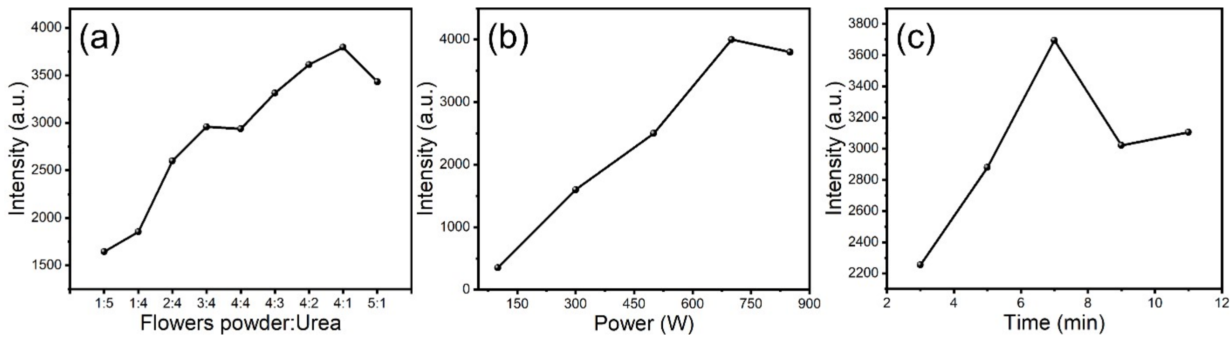

Fig. S2 Effect of reaction conditions on the fluorescence intensity of the synthesized B-CDs. mass ratio of *Bauhinia* flower powder and urea(a), reaction power(b), reaction time(c).

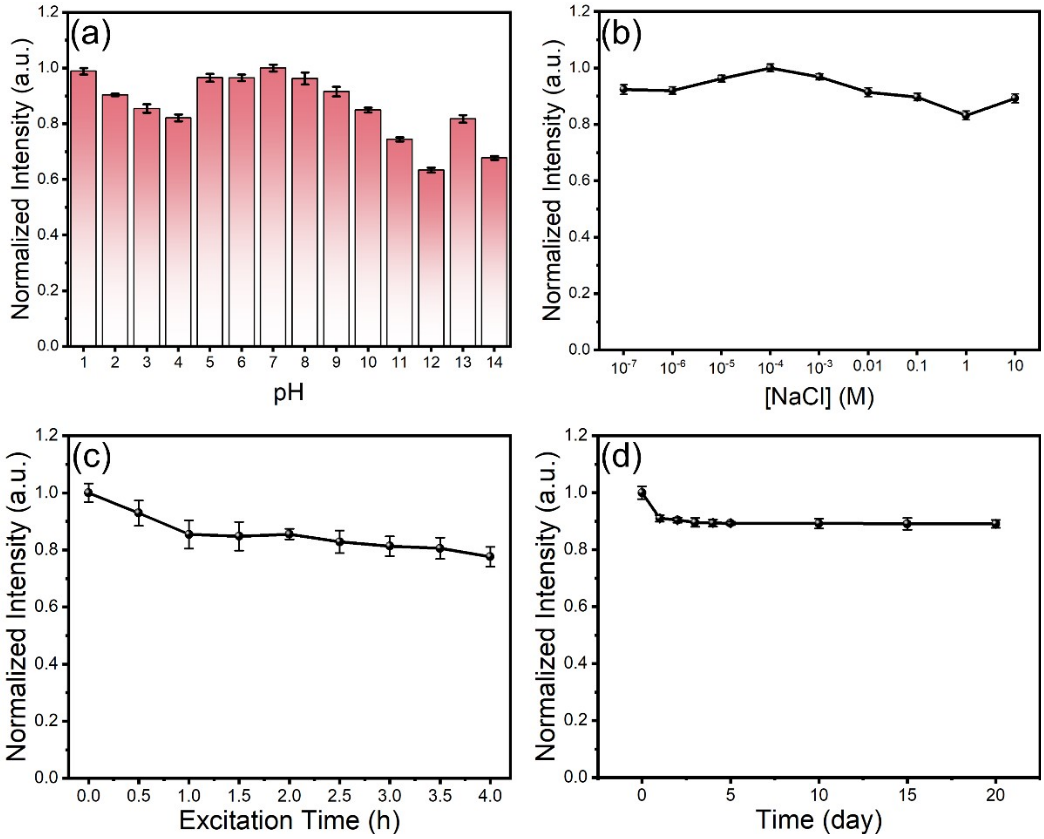

Fig. S3 Effect of pH (a), NaCl concentration (b), excitation time (b), and storage time (d) on FL intensity of RF-CDs (100 mg/L) under 365 nm excitation.

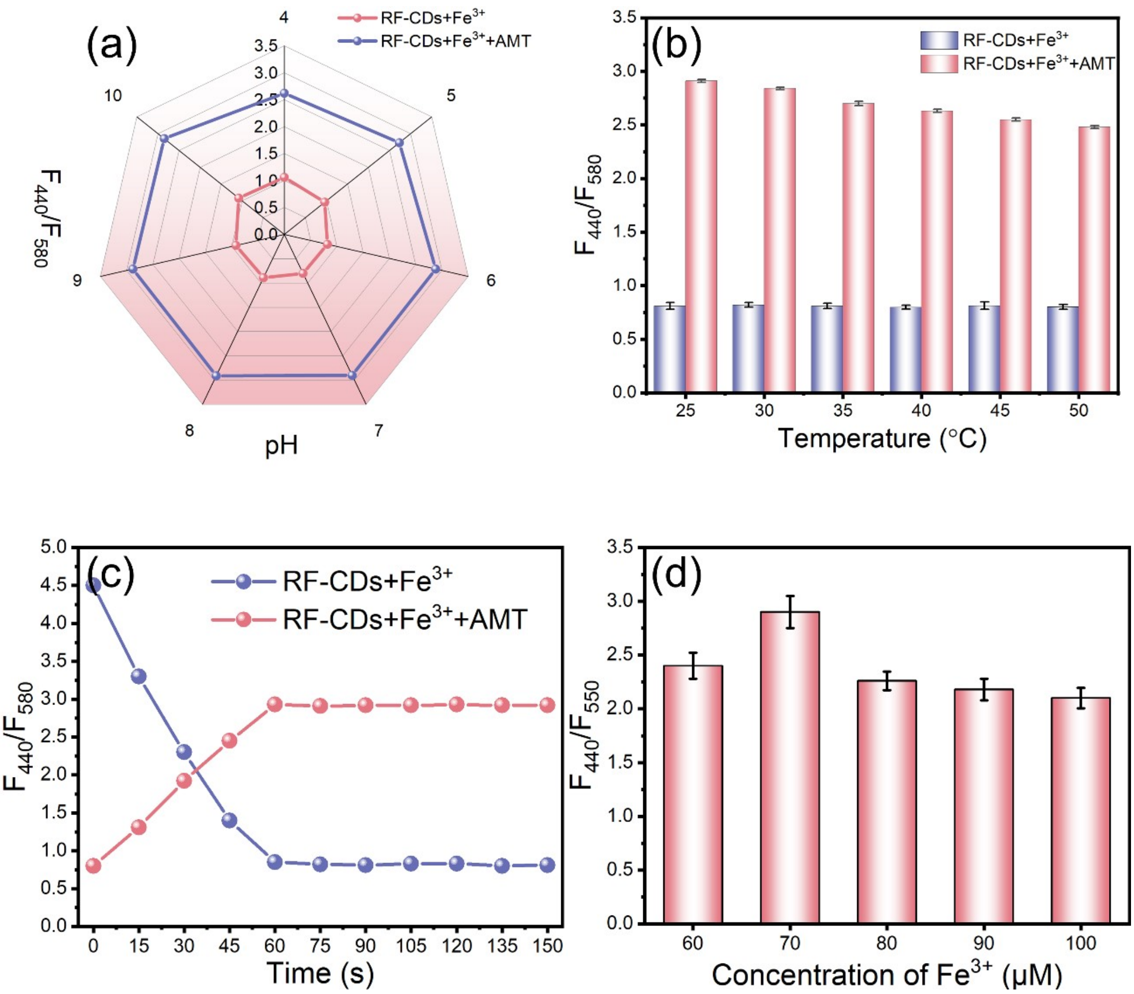

Fig. S4 Optimization of reaction conditions: pH (a), temperature (b), incubation time (c) and Fe^{3+} concentration (d).

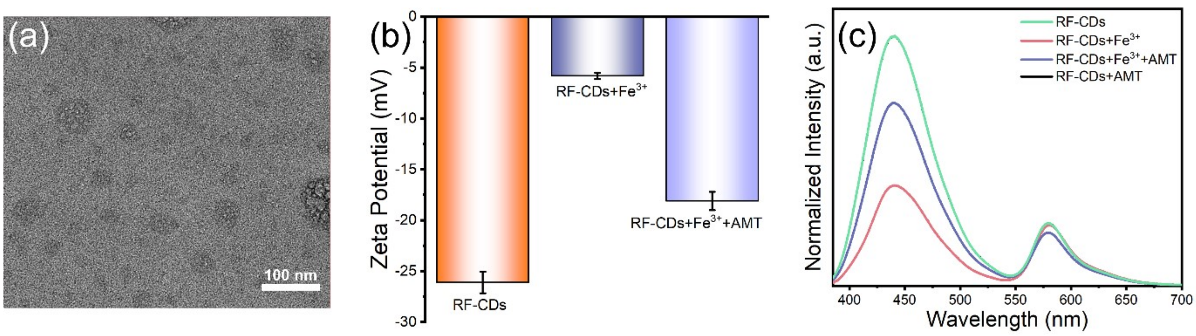

Fig. S5 (a) TEM image of RF-CDs after adding Fe^{3+}. (b) Zeta potentials of RF-CDs, RF-CDs+Fe^{3+}, RF-CDs+Fe^{3+}+AMT. (c) The fluorescence spectra of RF-CDs under different conditions.

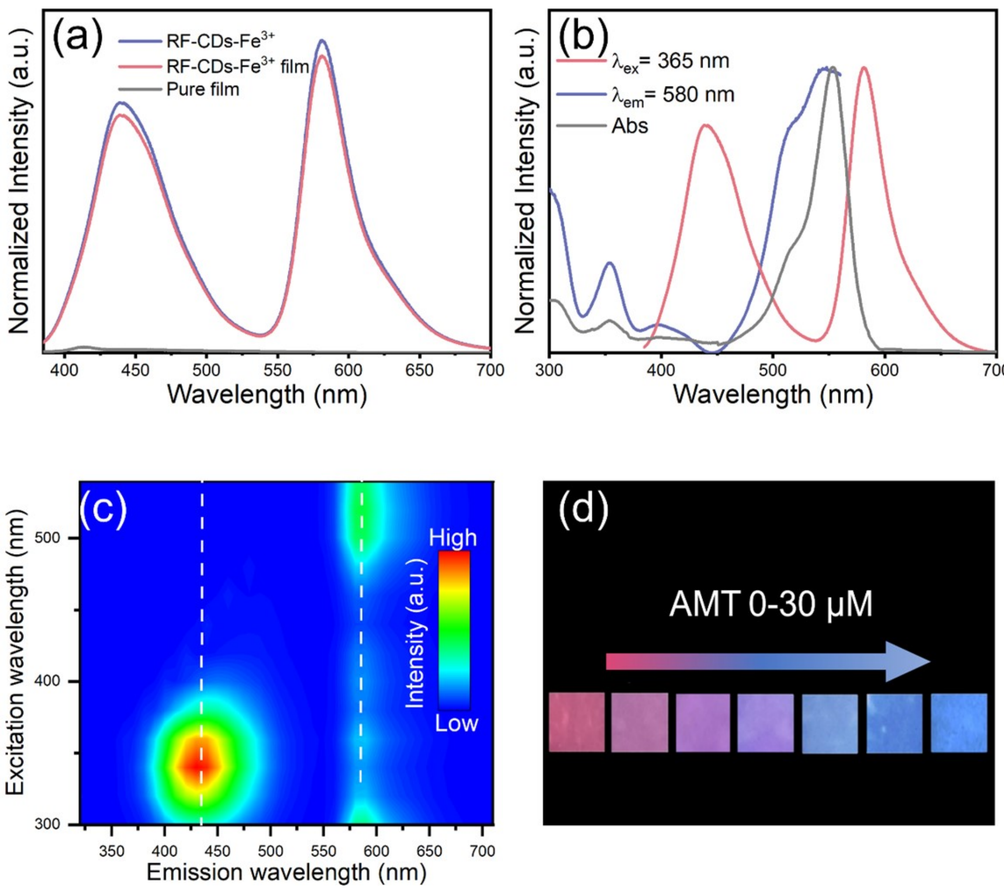

Fig. S6 The fluorescence spectra of RF-CDs-Fe^{3+}, RF-CDs-Fe^{3+} film and pure film (a), PL, PLE and UV-Vis spectra of RF-CDs-Fe^{3+} film (b), The fluorescence spectra of RF-CDs-Fe^{3+} film in different excitation wavelength (c), Fluorescence color change of RF-CDs-Fe^{3+} films with different AMT content (d).

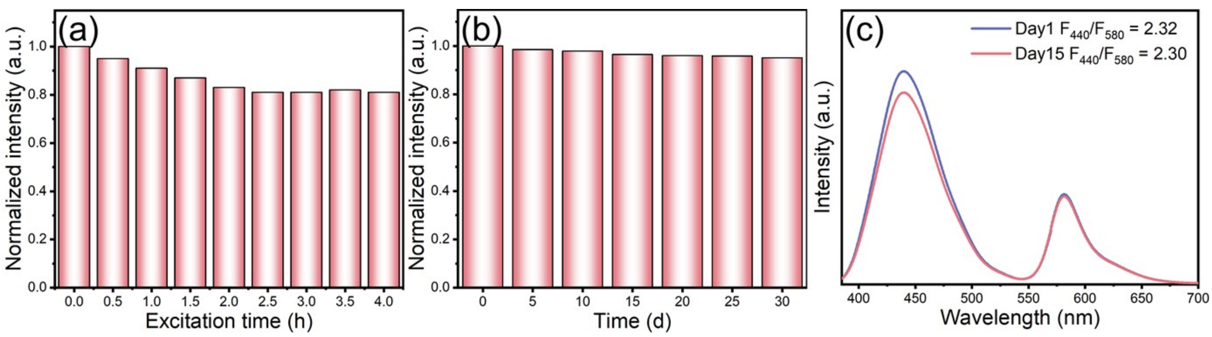

Fig. S7 Effect of excitation time (a), and storage time (b) on ratio of F_{440}/F_{580} of luminescent film under 365 nm excitation. (c) Fluorescence spectra of fluorescent films with storage times of 1 day and 30 days respectively when 30 μM AMT was added.

Supplemental Tables:

Table S1 Binding parameters and thermodynamic parameters of AMT and Fe^{3+}in aqueous solution.

T, K	**K_{AMT}**	**ΔH, kJ mol^{-1}**	**ΔS, J mol^{-1}K^{-1}**	**ΔG, kJ mol^{-1}**
293	**1.58×10^8**	**-55.02**	**27.3**	**-46.79**
300	**1.66×10^8**			**-46.91**

Table S2 Comparison of different CDs-based Fe^{3+} probes.

Fluorescent probes	CDs precursor	Linear range （μM）	Limit of detection （μM）	Ref
N-CDs	Citric acid，urea	0-60	0.802	2
N-CDs	Citric acid，o-phenylenediamine	0.5-90	0.37	3
GN-CDs	Gallic acid，o-Phenylenediamine	0-50	0.8	4
CMCQDs	Milk	0.1-20	0.6	5
LCDS	Mushroom	0-200	16	6
N-CDs	$C_6H_{12}N_4$，glucose	0-100	40.2	7
RF-CDs	*Bauhinia* flowers, urea	0-50	0.024	This work

References

1 S. Paydar, F. Feizi, M. Shamsipur, A. Barati, N. Chehri, A. (Arman) Taherpour and M. Jamshidi, *Sensors and Actuators B: Chemical*, 2022, **369**, 132243.

2 Z. Bian, Q. Xu, F. Chu, S. Hou, L. Xue, A. Hu, C. Dai, Y. Feng and B. Zhou, *J. Electron. Mater.*, 2024, **53**, 642–651.

3 Y. Zhao, L. Yu, Y. Deng, K. Peng and S. Huang, *Current Applied Physics*, 2023, **50**, 168–175.

4 S. Pang and S. Liu, *Analytica Chimica Acta*, 2020, **1105**, 155–161.

5 L. Zhang, B. Li, Y. Zhou, Y. Wu, T. Le and Q. Sun, *J Sol-Gel Sci Technol*, 2023, **106**, 173–185.

6 K. Klongklaw, B. Phiromkaew, P. Kiatsuksri, B. Kankit, S. Anantachaisilp and K. Wechakorn, *RSC Adv.*, 2023, **13**, 30869–30875.

7 P. Van Huan, *Luminescence*, 2024, **39**, e4852.